Negative index of refraction in artificial chiral materials

2006 J. Phys.: Condens. Matter 18 6883

(http://iopscience.iop.org/0953-8984/18/29/025)

INSTITUTE OF PHYSICS PUBLISHING JOURNAL OF PHYSICS: CONDENSED MATTER

J. Phys.: Condens. Matter **18** (2006) 6883–6890 doi:10.1088/0953-8984/18/29/025

Negative index of refraction in artificial chiral materials

Vassilios Yannopapas

Department of Materials Science, School of Natural Sciences, University of Patras, GR-26504 Patras, Greece

E-mail: vyannop@upatras.gr

Received 23 March 2006, in final form 30 May 2006
Published 6 July 2006
Online at stacks.iop.org/JPhysCM/18/6883

Abstract

A new class of negative refractive-index metamaterials made of metallic spheres arranged in a three-dimensional lattice of helicoidal symmetry is reported. The studied metamaterial possesses several frequency bands which give rise to negative refraction. The proposed structures constitute a viable solution to realizing optical metamaterials since they can exhibit negative refraction in the frequency region of the surface-plasmon excitations of noble metals.

(Some figures in this article are in colour only in the electronic version)

1. Introduction

Metamaterials are a new class of artificial electromagnetic (EM) materials which possess negative refractive index (NRI) in a certain frequency region. In such materials, the negative sign of the refractive index occurs when the effective permittivity ϵ_{eff} and the magnetic permeability μ_{eff} of the material become simultaneously negative [1, 2]. Most proposed NRI metamaterials slightly differ from the original proposal [3]: when a lattice of metallic split-ring resonators (SRRs) which possesses negative μ_{eff} over a frequency region is combined with a lattice of thin metallic wires possessing negative ϵ_{eff}, a window of negative refractive index occurs when both negative-ϵ_{eff} and negative-μ_{eff} regions overlap.

Recently, there has been suggested a new route for achieving NRI metamaterials by means of chirality [4–12]. The mechanism behind the creation of NRI bands in chiral media is simple: the dispersion relation in isotropic chiral media is given by [13] $k = (n \pm \kappa)\omega/c$, where n is the refractive index, κ corresponds to a chirality parameter, c the speed of light in vacuum, and ω the angular frequency. In the vicinity of a resonance of the electric permittivity and/ or magnetic permeability, the refractive index n may become smaller than the chirality parameter κ, and this way, the EM band associated with the minus sign of the dispersion relation corresponds to NRI (phase velocity opposite to the energy flow). However, as has been pointed out in [6, 10], the

material parameters required to achieve $\kappa > n$ (assuming no losses) are not met in naturally occurring materials and one has to introduce artificially manufactured materials instead [7, 10].

In the present work, an artificial chiral material is proposed which operates in the optical regime; it is based on Pendry's idea [7] of creating an NRI metamaterial through chirality: when a collection of resonant scatterers, e.g. of Drude or Lorentz type, is embedded in a chiral medium, then an NRI photon band occurs for one of the polarization modes. More specifically, if such scatterers are placed inside a non-chiral medium a hybridization-induced bandgap opens up [14]. Above this gap and at the centre of the Brillouin zone the photon states are triply degenerate (assuming cubic symmetry) as a doubly degenerate (of transverse nature) and a non-degenerate (of longitudinal nature) photon band coincide. When the medium hosting the scatterers is chiral, the doubly degenerate (transverse) band above the gap splits into two non-degenerate bands creating the NRI part of the dispersion relation [7]. As a resonant chiral structure, Pendry suggested a chiral version of the original Swiss roll structure [15], where the chiral Swiss rolls are created by winding a continuous metal foil onto a cylinder so that an overlapping helix is formed. Due to the elaborate shape of the Swiss rolls, such structures can only be realized in the MHz regime [15]. In this paper, a chiral resonant structure is proposed where chirality does not stem from the shape of the scatterers but from their positioning in space.

2. Resonant spheres in a chiral medium

The scope of the present paper is to enquire about the possibility of realizing an NRI metamaterial in the form of an artificial chiral structure of resonant spheres. The first approach in this direction is an effective medium description of the EM response of such a structure. Namely, the calculation of the dispersion relations will reveal the conditions under which an NRI band can occur. The constitutive relation in a chiral material is stated as [16]

$$\mathbf{D} = \hat{\epsilon}\mathbf{E} + \mathrm{i}\gamma\mathbf{E}\times\mathbf{k} \tag{1}$$

where $\hat{\epsilon}$ is the permittivity tensor

$$\hat{\epsilon} = \begin{pmatrix} \epsilon_\parallel & 0 & 0 \\ 0 & \epsilon_\parallel & 0 \\ 0 & 0 & \epsilon_\perp \end{pmatrix} \tag{2}$$

$\mathbf{k}$ is the wavevector, $\mathbf{D}$ the electric displacement and $\mathbf{E}$ the electric field. γ is the gyrotropic parameter. The second term of equation (1) describes the spatial dispersion of the chiral medium. Because of this term, it is not necessary to write down the corresponding expression for the magnetic field $\mathbf{H}$ [12, 16]. For plane waves, Maxwell equations yield

$$\mathbf{D} = \frac{k^2c^2}{\omega^2}[\mathbf{E} - \mathbf{k}(\mathbf{k}\cdot\mathbf{E})/k^2]. \tag{3}$$

If we consider transverse plane waves, i.e. $\mathbf{k}\cdot\mathbf{E} = 0$ in equation (3), we may take, without loss of generality, that $\mathbf{E} = (E_x, E_y, 0)$ and $\mathbf{k} = (0, 0, k)$, and then substitute them in equations (1) and (3). This results in the following homogeneous system of linear equations:

$$\begin{aligned} &D_x - \epsilon_\parallel E_x - \mathrm{i}\gamma k E_y = 0 \\ &D_y - \epsilon_\parallel E_y + \mathrm{i}\gamma k E_x = 0 \\ &D_x - (k^2c^2/\omega^2)E_x = 0 \\ &D_y - (k^2c^2/\omega^2)E_y = 0. \end{aligned} \tag{4}$$

For nontrivial solutions of equation (4), the corresponding determinant should vanish, giving the following dispersion relation of the chiral material:

$$\epsilon_\parallel(\omega) - \frac{c^2k^2}{\omega^2} = \pm\gamma k. \tag{5}$$

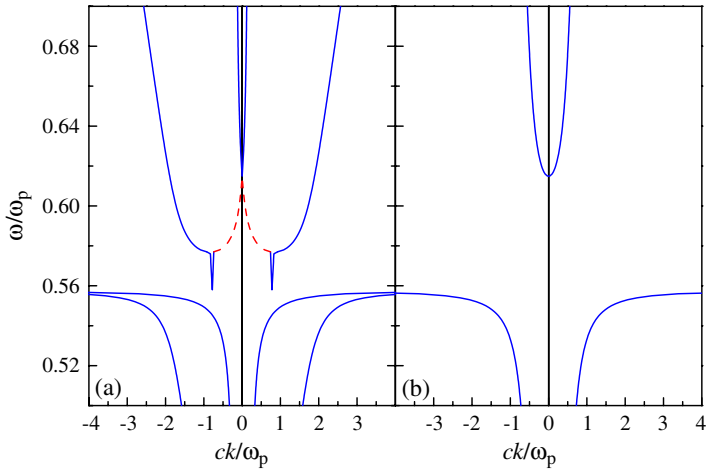

Figure 1. (a) Effective medium dispersion relations for a collection of Drude spheres embedded in a chiral medium, with volume filling fraction $f = 0.067$ and gyrotropic parameter $\gamma\omega_p/c = 5$. (b) The same as in (a) but for a material without chirality ($\gamma\omega_p/c = 5$).

Solving for the wavenumber k we obtain the following four solutions:

$$k = \frac{\pm\gamma\omega^2 \pm \omega\sqrt{4c^2\epsilon_\parallel(\omega) + \gamma^2\omega^2}}{2c^2}. \tag{6}$$

If $\epsilon_\parallel(\omega)$ supports a longitudinal excitation, i.e. if there is a frequency ω_L such that $\epsilon_\parallel(\omega_L) = 0$ while, at the same time, $d\epsilon_\parallel/d\omega > 0$ at ω_L, an NRI frequency region may develop around this frequency [5, 7, 12]. Such excitations are met, e.g., in Drude or Drude–Lorentz types of electric permittivity. In our case of study, i.e. a collection of resonant spheres in a chiral medium, $\epsilon_\parallel(\omega)$ can be obtained by the Maxwell–Garnett effective medium approximation. Namely, $\epsilon_\parallel(\omega) = \epsilon_{eff}$ where the effective permittivity ϵ_{eff} is given by the Clausius–Mossotti formula [17]

$$\frac{\epsilon_{eff} - \epsilon_h}{\epsilon_{eff} + 2\epsilon_h} = f\frac{\epsilon_s - \epsilon_h}{\epsilon_s + 2\epsilon_h} \tag{7}$$

where ϵ_s is the permittivity of the resonant spheres, ϵ_h the permittivity of the chiral material hosting the spheres and f the volume filling fraction. The permittivity of the spheres is assumed to be of Drude type without losses

$$\epsilon(\omega) = 1 - \omega_p^2/\omega^2 \tag{8}$$

where ω_p stands for the bulk plasma frequency. As is well known the above type of dielectric function describes satisfactorily the optical response of noble metals. The permittivity of the chiral medium is taken to be unity ($\epsilon_h = 1$ in equation (7)). The volume filling fraction is taken relatively low, $f = 0.067$, and the gyrotropic parameter $\gamma\omega_p/c = 5$. The permittivity as given by equations (7) and (8) possesses two real roots, one of which corresponds to positive $d\epsilon_{eff}/d\omega$, and therefore an NRI is expected to appear around it. These roots have their origin in the surface plasmon resonances of the individual plasma spheres [14]. Figure 1(a) shows the dispersion relation (6) for the above parameters. One clearly identifies a frequency band (broken (red) line of figure 1(a)) from $\omega/\omega_p = 0.577$ to 0.615, where the group velocity is negative as frequency decreases monotonically with the wavevector. By definition, this band is an NRI frequency band corresponding to waves of one type of handedness. The dips in the

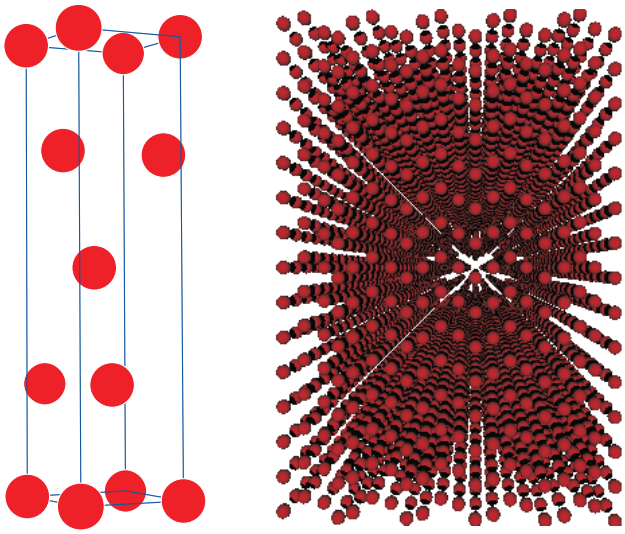

(a) (b)

Figure 2. Artificial chiral crystal. (a) Unit cell of a tetragonal crystal consisting of four non-primitive planes of spheres parallel to the (001) surface at positions $(0, 0, 0)$, $(b, 0, d/4)$, $(b, b, d/2)$, and $(0, b, 3d/4)$, with $b = 0.3a$ and $d = 2a$. (b) Finite slab of the crystal.

dispersion relation correspond to regions where the square root of equation (6) is negative and therefore k is complex. In order to establish the fact that the appearance of the NRI band is a result of the chirality (chirality-induced frequency band), in figure 1(b) I show the dispersion relation for zero chirality ($\gamma = 0$). It is clear that no NRI band occurs although all the other effective medium parameters are the same as in figure 1(a). Note that, not only for zero, but even for non-zero but small enough values of $\gamma\omega_p/c$, the chirality-induced NRI band may also disappear.

3. Artificial chiral structure

As predicted by the effective-medium approach of the previous section, a chiral medium in which Drude-type spheres are embedded can exhibit an NRI frequency band around a longitudinal excitation of the effective electric permittivity. In this section, we propose a new artificial chiral structure which exhibits NRI behaviour and is essentially a crystal of Drude-type spheres in helical configuration. This structure cannot be directly described by the effective-medium model presented in the previous section as the latter corresponds to an array of spheres embedded in a chiral medium; in the proposed chiral structure, no naturally occurring chiral material is involved; chirality originates from the positioning of the Drude spheres in space and a rigorous numerical method has been employed for the study of the artificial structure (see below). The crystal is shown in figure 2 and can be described as a tetragonal crystal with a four-point basis. The crystal is viewed as a succession of planes of spheres parallel to the xy-plane. Each plane possesses the same 2D periodicity defined by the primitive vectors $\mathbf{a}_1 = (a, 0, 0)$ and $\mathbf{a}_2 = (0, a, 0)$ ((001) crystallographic surface). A unit layer of the crystal consists of four non-primitive planes of spheres at $(0, 0, 0)$, $(b, 0, d/4)$, $(b, b, d/2)$, and $(0, b, 3d/4)$. The $(n + 1)$th unit layer is obtained from the nth layer by the primitive translation $\mathbf{a}_3 = (0, 0, d)$. Such a structure (one with dielectric spheres) was originally suggested by Karathanos *et al* [18] as an artificial chiral material which can be used for rotating the plane of polarization of

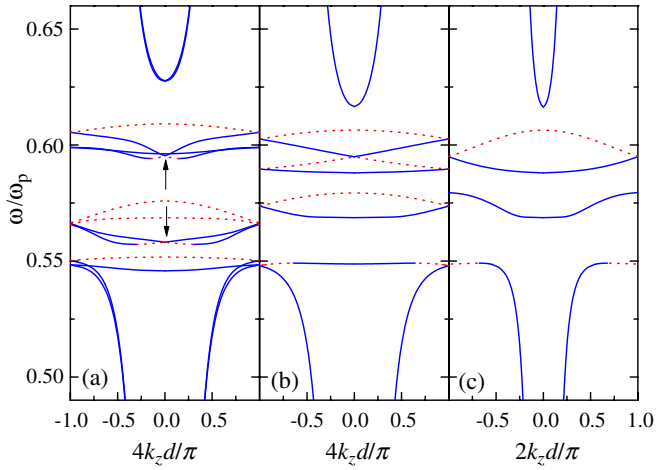

Figure 3. (a) Frequency band structure normal to the (001) surface of the chiral crystal of figure 2. The broken (red) lines correspond to NRI bands and the solid (blue) ones to bands of positive refractive index. The broken (red) lines marked by the arrows correspond to chirality-induced NRI bands. (b) The same as in (a) but for a (non-chiral) tetragonal crystal with $b = 0.5a$ and $d = 2a$. (c) The same as in (b) but for a tetragonal crystal with unit layer consisting of two non-primitive planes of spheres at $(0, 0, 0)$ and $(b, 0, d/4)$, with $b = 0.5a$ and $d = 2a$.

linearly polarized light. The spheres of the crystal of figure 2 are of radius $S = 0.2a$ and their dielectric function is of Drude type. The lattice constant a of the 2D square lattice is taken to be $a = c/\omega_p$. For example, for gold $\hbar\omega_p = 8.99$ eV and therefore the lattice constant is $a = 22$ nm and the radius of the spheres $S = 4.4$ nm. Losses are turned off by setting $\tau^{-1} = 0$ in equation (8). Note that, as pointed out in the previous section, this particular choice of dielectric function is not essential for the occurrence of NRI; other types of dielectric function such as the Drude–Lorentz type (ionic materials) describing the phonon–polariton excitation are also expected to reproduce the findings of this work.

In order to discover NRI frequency regions for the crystal of figure 2(a) frequency band structure calculation is needed. This is done by using a photonic version of the layer Korringa–Kohn–Rostoker (LKKR) method, which is based on an *ab initio* multiple scattering theory, using a well documented computer code [19, 20]. Figure 3(a) shows the frequency band structure, for $\mathbf{k}_\parallel = \mathbf{0}$ (normal to the (001) surface), of the crystal of figure 2 with $b = 0.3a$ and $d = 2a$. The calculation is carried out in the dipole approximation ($l_{max} = 1$ in the spherical-wave expansion of the EM field) with 29 reciprocal-lattice vectors (in the plane-wave expansion of the EM field) taken into account. All bands appearing in figure 3(a) are non-degenerate due to the chiral symmetry of the crystal. One identifies six frequency bands corresponding to NRI. The first NRI band extends from $\omega/\omega_p = 0.55$ to 0.552, the second from 0.557 to 0.558, the third from 0.566 to 0.568, the fourth from 0.566 to 0.576, the fifth from 0.594 to 0.595 and the sixth from 0.605 to 0.609. As expected, the NRI frequencies are developed around the surface plasma modes of a single Drude nanosphere; as a result, the NRI bands lie in the optical regime since the surface plasma frequency $\omega_{sp} = \omega_p/\sqrt{3}$ of noble metal nanoparticles lies in this frequency region. The corresponding effective refractive index $n_{eff} = -ck_z/\omega$ for each of the frequency bands of figure 3(a) is shown in figure 4. Although one observes frequency regions where the crystal exhibits birefringence (different values of the refractive index for waves of opposite handedness), there also exist regions where only NRI bands exist. By inspecting the shape of the NRI bands and comparing them with that of figure 2, it is evident that the second

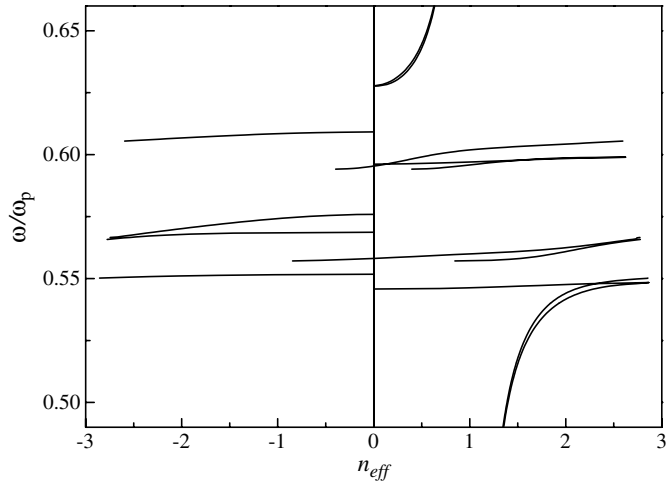

Figure 4. Effective refractive index $n_{\text{eff}} = -ck_z/\omega$ corresponding to the frequency bands of figure 3(a).

and the fifth band (broken (red) lines marked by the arrows in figure 3(a)) are chirality-induced bands. Indeed, figure 3(b) depicts the frequency band structure for a crystal with the same parameters as that of figure 3(a), except that $b = 0.5a$ is chosen instead of $b = 0.3a$. In this case, the crystal no longer exhibits chirality. It is obvious that the second and fifth NRI bands of figure 3(a) disappear along with the chiral symmetry of the crystal. However, one can still identify three NRI frequency bands and a partially NRI band. Note that, although the scatterers of the crystal of figure 3(b) are still positioned in a helicoidal configuration, the presence of both right- and left-handed helices does not allow for rotation of the polarization vector and hence chirality is lost [18]. The non-chiral crystal of figure 3(b) is described in the same way as the chiral crystal of figure 3(a) is described, i.e as a tetragonal crystal with a four-point basis. However, this crystal possesses a simpler structure and can be described by a tetragonal crystal with a two-point basis with spheres at $(0, 0, 0)$, $(b, 0, d/4)$, with $b = 0.5a$ and $d = 2a$ (note in passing that for $d = \sqrt{2}a$ the resulting crystal structure is that of diamond). Using this crystal basis, the frequency band structure is recalculated and shown in figure 3(c). One observes that none of the NRI bands survive except from the sixth band of figure 3(a), which, by the way, appears to be substantially wider (it extends from $\omega/\omega_{\text{p}} = 0.595$ to 0.606). However, this band is non-degenerate and therefore does not couple with normally incident light. The NRI bands which appear in both figures 3(a) and (b) but not reproduced in figure 3(c) must stem from a band-folding effect caused by the consideration of a four-point basis in figure 3(b) instead of a two-point basis in figure 3(c).

The wavelength-to-structure ratio of the crystal of figure 3(a) is $\lambda/d = 5.3$ for the frequency $\omega/\omega_{\text{p}} = 0.6$, rendering the crystal a truly subwavelength metamaterial. The refractive index curves of figure 4 correspond to $\mathbf{k}_{\parallel} = \mathbf{0}$ ($\bar{\Gamma}$-point of the (001) surface Brillouin zone (SBZ)), and more or less, to nonzero values of $\mathbf{k}_{\parallel}$ around the $\bar{\Gamma}$-point. Due to the subwavelength nature of the proposed metamaterial, the range of possible incident angles (0°–90°) corresponds to a small $\mathbf{k}_{\parallel}$-area of the SBZ around the $\bar{\Gamma}$-point. Therefore, the frequency band structure of figure 3(a) and the refractive index of figure 4 will remain practically the same for off-normal incidence.

So far, calculations have been carried out assuming only dipole interactions ($l_{\max} = 1$) between the spheres. In order to explore the role of higher-multipole interactions between the

spheres, the calculation of the frequency band structure of figure 3(a) has been repeated for angular-momentum cut-off $l_{\max} = 2$ and for the same number (29) of reciprocal-lattice vectors (which ensured convergence of the plane-wave expansion of the EM field). There are new bands generated for $\omega/\omega_p > 0.61$ which are of quadrupole origin ($l_{\max} = 2$). Fortunately, these quadrupole bands do not mix with the dipole ones, leaving the NRI bands almost intact apart from a shift of the NRI bands to lower frequencies and a relative decrease of their bandwidth. However, this picture changes drastically when the spheres are closer to each other, e.g. in the close-packed arrangement allowed by the specific tetragonal lattice with a basis. In this case, the quadrupole bands become wider and overlap with the already extended dipole bands and subsequently with the NRI bands, obscuring the observation of negative refraction. Note that when the actual dielectric function of a noble metal is employed (meaning also that the actual losses of the metal particles are taken into account) the role of higher-multipole interaction is diminished, rendering the dipole modes as the leading contribution to the EM field [14].

4. Outlook and conclusion

A final note on the realization of the metamaterials proposed in this work. The fabrication of a chiral tetragonal crystal of metal particles is surely a challenging task since three-dimensional arrays of metal particles have not been reported so far, apart from arrays of metal-coated silica opal structures [21]. Such structures, i.e. with metal-coated spheres arranged with the proposed chiral symmetry, could equally serve the purpose of realizing an NRI metamaterial, since metal-coated spheres exhibit strong surface plasmon resonances like purely metallic spheres but for lower frequencies. However, it is not restrictive to use arrays of metallic particles in order to realize an artificial chiral material. Recent advances in holographic lithography have made plausible the realization of a chiral dielectric photonic crystal [22]: a three-dimensional, periodic chiral interference pattern of laser beams is used to expose photoresist. The remaining structure is infiltrated with a high-refractive index dielectric in order to achieve large frequency gaps. If metal such as gold or silver is used instead of dielectric, the resulting chiral crystal is expected to exhibit NRI bands similar to those of the tetragonal chiral crystals of spherical scatterers described in this work.

In conclusion, I have shown that Drude-type particles occupying the sites of crystal with chiral symmetry exhibit a rich spectrum of NRI bands. The proposed artificial structures are truly subwavelength metamaterials with wavelength-to-structure ratio as high as 5:1. They can exhibit negative refraction in the optical region as the latter is a result of the surface plasmon resonances of the individual Drude particles (which occur in the optical regime for noble-metal particles) and the chiral symmetry of the crystal.

Acknowledgment

This work was supported by the ‘Karatheodory’ research fund of the University of Patras.

References

[1] Veselago V G 1968 *Sov. Phys.—Usp* **10** 509
[2] Pendry J B 2000 *Phys. Rev. Lett.* **85** 3966
[3] Shelby R A, Smith D R and Schultz S 2001 *Science* **292** 77
[4] Lakhtakia A 2002 *Microw. Opt. Technol. Lett.* **33** 96
[5] Tretyakov S, Nefedov I, Shivola A, Maslovski S and Simovski C 2003 *J. Electromagn. Waves Appl.* **17** 695
[6] Mackay T G and Lakhtakia A 2004 *Phys. Rev.* E **69** 026602

[7] Pendry J B 2004 *Science* **306** 1353
[8] Mackay T G and Lakhtakia A 2005 *New J. Phys.* **7** 165
[9] Monzon C and Forester D W 2005 *Phys. Rev. Lett.* **95** 123904
[10] Tretyakov S, Shivola A and Jylhä L 2005 *Photon. Nanostruct.* **3** 107
[11] Shen J Q 2006 *Phys. Rev.* B **73** 045113
[12] Agranovitch V M, Garstein Yu N and Zakhidov A A 2006 *Phys. Rev.* B **73** 045114
[13] Lindell I V, Shivola A H, Tretyakov S A and Viitanen A J 1994 *Electromagnetic Waves in Chiral and Bi-Isotropic Media* (Norwood: Artech House)
[14] Yannopapas V, Modinos A and Stefanou N 1999 *Phys. Rev.* B **60** 5359
[15] Wiltshire M C K, Hajnal J V, Pendry J B, Edwards D J and Stevens C J 2003 *Opt. Express* **11** 709
[16] Landau L D and Lifshitz E M 1984 *Electrodynamics of Continuous Media* (Oxford: Butterworth-Heinemann)
[17] Jackson J D 1975 *Classical Electrodynamics* (New York: Wiley)
[18] Karathanos V, Stefanou N and Modinos A 1995 *J. Mod. Opt.* **42** 619
[19] Stefanou N, Yannopapas V and Modinos A 1998 *Comput. Phys. Commun.* **113** 49
[20] Stefanou N, Yannopapas V and Modinos A 2000 *Comput. Phys. Commun.* **132** 189
[21] Jiang Y, Whitehouse C, Li J, Tam W Y, Chan C T and Sheng P 2003 *J. Phys.: Condens. Matter* **15** 5871
[22] Dedman E R, Sharp D N, Turberfield A J, Blanford C F and Denning R G 2005 *Photon. Nanostruct.* **3** 79